Journal of Cell Science

PERP regulates enamel formation via effects on cell–cell adhesion and gene expression

Andrew H. Jheon[1], Pasha Mostowfi[1], Malcolm L. Snead[2], Rebecca A. Ihrie[3], Eli Sone[4], Tiziano Pramparo[5], Laura D. Attardi[6] and Ophir D. Klein[1,5,*]

[1]Department of Orofacial Sciences and Program in Craniofacial and Mesenchymal Biology, University of California, San Francisco, CA 94143, USA
[2]Center for Craniofacial Molecular Biology, University of Southern California, 2250 Alcazar Street – CSA 103, Los Angeles, CA 90033, USA
[3]Department of Neurological Surgery and Institute for Regeneration Medicine, University of California, San Francisco, 35 Medical Center Way, RMB933, San Francisco, CA 94143-0525, USA
[4]Faculty of Dentistry, Department of Materials Science and Engineering, and Institute of Biomaterials and Biomedical Engineering, University of Toronto, M5S 3G9, Canada
[5]Department of Pediatrics and Institute for Human Genetics, University of California, San Francisco, CA 94143, USA
[6]Departments of Radiation Oncology and Genetics, Stanford University, Palo Alto, CA 94305-5101, USA
*Author for correspondence (ophir.klein@ucsf.edu)

Summary

Little is known about the role of cell–cell adhesion in the development of mineralized tissues. Here we report that PERP, a tetraspan membrane protein essential for epithelial integrity, regulates enamel formation. PERP is necessary for proper cell attachment and gene expression during tooth development, and its expression is controlled by P63, a master regulator of stratified epithelial development. During enamel formation, PERP is localized to the interface between the enamel-producing ameloblasts and the stratum intermedium (SI), a layer of cells subjacent to the ameloblasts. *Perp*-null mice display dramatic enamel defects, which are caused, in part, by the detachment of ameloblasts from the SI. Microarray analysis comparing gene expression in teeth of wild-type and *Perp*-null mice identified several differentially expressed genes during enamel formation. Analysis of these genes in ameloblast-derived LS8 cells upon knockdown of PERP confirmed the role for PERP in the regulation of gene expression. Together, our data show that PERP is necessary for the integrity of the ameloblast–SI interface and that a lack of *Perp* causes downregulation of genes that are required for proper enamel formation.

Key words: PERP, P63, Amelogenesis, Ameloblast, Stratum intermedium, Cell–cell adhesion, Desmosomes

Introduction

PERP (P53 apoptosis effector related to PMP-22) is a tetraspan membrane protein that has an essential role in the epithelial integrity of a number of tissues (Ihrie et al., 2005). *Perp* was identified in mouse embryonic fibroblasts and found to be a mediator of tumor suppressor *Tp53*-dependent apoptosis in several cell types (Attardi et al., 2000; Ihrie et al., 2003), and it is a direct target of the P53 paralog tumor protein P63, which is crucial for the morphogenesis of skin and its associated structures, including hair and teeth (Ihrie et al., 2005; Laurikkala et al., 2006; Senoo et al., 2007; Yang et al., 1998). PERP has been shown to have an essential role in the stable assembly of desmosomes (Ihrie et al., 2005). *Perp*-null mice display blisters in their epithelia as well as features of ectodermal dysplasia syndromes (Ihrie et al., 2006) in which patients present with abnormal development of ectoderm-derived tissues such as skin, hair and teeth (Freire-Maia, 1971).

The outer layer of teeth is composed of enamel, which is the hardest substance in the mammalian body and is unique among mineralized tissues in its epithelial origin. Defects in enamel formation result in amelogenesis imperfecta, a group of autosomal-dominant, autosomal-recessive or X-linked inherited disorders (for a review, see Fleischmannova et al., 2008; Hu et al., 2007; Stephanopoulos et al., 2005). Enamel formation, or amelogenesis, is initiated as the epithelial-derived enamel organ (EO) generates the inner enamel epithelium (IEE), which differentiates into the enamel-forming ameloblasts. The life cycle of ameloblasts involves

several stages (Smith and Nanci, 1995). First, the presecretory ameloblasts differentiate into secretory ameloblasts, which deposit an extracellular matrix comprising proteins such as amelogenin, ameloblastin, enamelin, tuftelin and matrix metalloproteinase-20 (MMP-20) (Hu et al., 2007; MacDougall et al., 1998; Stephanopoulos et al., 2005), and mineralization is initiated. A shift from matrix deposition to resorption occurs at the transitional and mature stages as MMP-20, kallikrein-4 (Hu et al., 2007; Stephanopoulos et al., 2005), amelotin (Iwasaki et al., 2005; Moffatt et al., 2006) and Odam (Moffatt et al., 2008) are predominantly expressed. At the mature stage, the matrix is replaced by secondary crystal growth, leading to the complete mineralization of enamel. During the progression of these stages, the basal surface of ameloblasts is attached to the stratum intermedium (SI) (Hay, 1961; Sasaki et al., 1984). The SI and stellate reticulum (SR) layers fuse to form the papillary layer at the transitional and mature stages. Hereafter, the papillary layer will be referred to as the SI. Finally, as the tooth erupts, the cells derived from the EO, namely the SI, SR, outer enamel epithelium (OEE), and ameloblasts, are sloughed off, and the uncovered enamel is devoid of cells and organic matrix.

Little is known regarding the role of cell–cell adhesion and desmosomes during tooth development. Desmosomes are transmembrane, macromolecular complexes that provide strong cell–cell adhesion and are anchored to intermediate filaments (for a review, see Franke, 2009; Garrod and Chidgey, 2008; Green and

Simpson, 2007; Jamora and Fuchs, 2002; Owen and Stokes, 2010; Thomason et al., 2010). Desmosomes consist of members of at least three distinct protein families: the cadherins, such as desmogleins and desmocollins, the armadillo proteins, including plakoglobin and the plakophilins, and the plakins. Previous studies have shown the localization of desmosomal proteins in the EO and EO-derived cells of incisors and molars (Fausser et al., 1998; Kieffer-Combeau et al., 2001), and putative roles for desmosomes in morphogenesis and positioning of the molars have been proposed (Cam et al., 2002; Lesot et al., 2002). Recently, the adherens junction protein nectin-1 was shown to indirectly affect desmosomes at the ameloblast–SI interface, resulting in enamel defects (Barron et al., 2008). In both human diseases and mouse models in which components of desmosomes are mutated or knocked out, failure of cell–cell adhesion causes epithelial blistering and fragility in the presence of mechanical stress (for a review, see Green and Simpson, 2007; Jamora and Fuchs, 2002; Sonnenberg and Liem, 2007; Thomason et al., 2010).

Because PERP is required for desmosome assembly and for the integrity of stratified epithelia, we set out to determine whether PERP has a role in the formation of enamel. Here, we report that PERP regulates amelogenesis through its effects on cell–cell adhesion and on gene regulation.

Results

Perp is expressed in embryonic teeth and its expression is regulated by P63

The expression profiles of PERP, the desmosomal component desmokplakin (DSP) and P63 were analyzed in developing first upper molars by immunofluorescence staining (Fig. 1C–F′,I–L′). In previous experiments using keratinocytes, PERP was shown to colocalize with desmosomes and its expression was regulated by P63 (Ihrie et al., 2005). In the oral cavity, we found similar immunofluorescence staining of PERP and DSP in the oral and tongue epithelia, and the skin (supplementary material Fig. S1). In the developing tooth, anti-PERP antibody staining was detected throughout the dental epithelium at embryonic day (E) 14.5 (Fig. 1C), and by E16.5, expression was localized to the developing EO-derived cells, namely the IEE, SI, SR and OEE (Fig. 1I). DSP showed a similar expression profile to PERP (Fig. 1D,J), and the merged images showed colocalization of PERP and DSP (Fig. 1E,K). Higher magnification images showed colocalization of PERP and DSP in the EO at E14.5 and predominantly in the SI and SR, with some expression in the IEE at E16.5 (Fig. 1C′–E′,I′–K′). As previously reported (Casasco et al., 2006; Laurikkala et al., 2006; Rufini et al., 2006), P63 was localized to the nuclei of EO and EO-derived cells at E14.5 and E16.5 (Fig. 1F,F′,L,L′). Thus, P63, DSP and PERP are co-expressed during tooth development.

To test whether P63 regulates *Perp* expression during amelogenesis, we performed luciferase reporter assays (Fig. 1M) using the ameloblast-like LS8 cell line, which was derived from murine EO epithelium (Chen et al., 1992; Xu et al., 2006). LS8 cells were isolated from the enamel epithelial organ of embryonic mouse teeth during the amelogenesis process. These cells express many of the genes specific for amelogenesis, such as ameloblastin, amelogenin and enamelin, at sufficiently high levels that they have been used for many in vitro studies of amelogenesis, including gene promoter analysis (Dhamija et al., 1999; Zhou et al., 2000;
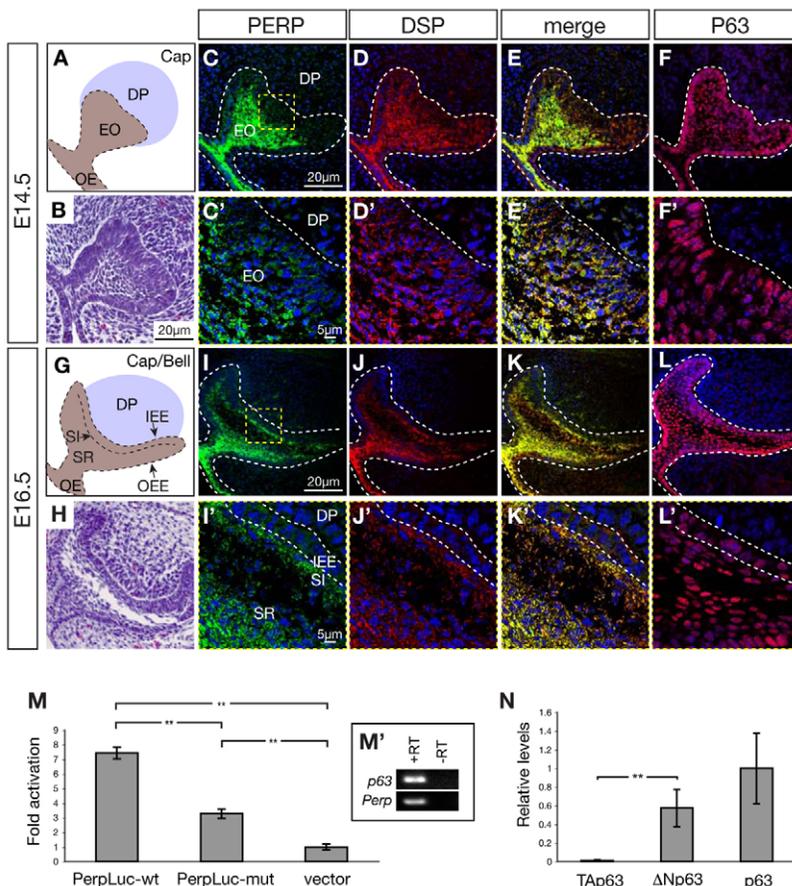

Fig. 1. **PERP is expressed in developing teeth and is regulated by P63.** (**A**,**G**) Cartoon of the cap and bell stages during molar development. At the cap stage, the enamel organ (EO) forms and surrounds the dental papilla (DP). At the bell stage, the EO begins to differentiate into the inner enamel epithelium (IEE), which generates the future ameloblasts, as well as the stratum intermedium (SI), stellate reticulum (SR), and the outer enamel epithelium (OEE). (**B**,**H**) H&E staining of coronal sections of molars at E14.5 and E16.5. (**C–E**,**I–K**) Double immunofluorescence staining and merge of PERP and desmoplakin (DSP). Higher magnification images show colocalization of PERP and DSP in the EO at E14.5 (C′–E′) and in the SI, SR and IEE at E16.5 (I′–K′). (**F**,**F′**,**L**,**L′**) Immunofluorescence staining of P63 shows overlapping expression profile with that of PERP and DSP. (**M**) Luciferase assays in ameloblast-like LS8 cell line using empty vector (vector), the *Perp* promoter and intron containing a P63-responsive element (PerpLuc-wt), or a construct with a mutated P63-responsive element (PerpLuc-mut). (**M′**) Inset shows the endogenous expression of *Tp63* and *Perp* in LS8 cells detected by PCR with (+RT) or without (–RT) reverse transcription. (**N**) qPCR analysis showing relative expression levels of the various P63 isoforms, N-terminal transcriptional activation (TAp63), N-terminal truncated (ΔNP63) or pan p63. ******$P<0.01$.

Zhou and Snead, 2000). Recently, these cells have been shown to respond to peptide amphiphiles by producing an enamel extracellular matrix that is similar to authentic enamel (Huang et al., 2008). Constructs in which luciferase expression was driven by the wild-type *Perp* promoter and intron 1, which contains a P63-responsive element (PerpLuc-wt), or with a mutated P63-responsive element (PerpLuc-mut) (Reczek et al., 2003) were transfected into LS8 cells, which express endogenous *Tp63* and *Perp* (Fig. 1M′). We found that the *Perp* reporter was transactivated through the P63-responsive element, as evidenced by the decrease in luciferase activity with PerpLuc-mut compared with PerpLuc-wt (Fig. 1M). Interestingly, PerpLuc-mut constructs showed higher transcriptional activity than the empty vector, pointing to the involvement of additional transactivators other than P63 and/or additional regulatory sites in the regulation of *Perp* expression.

P63, a member of the P53 protein family, is expressed as six isoforms as a result of alternative transcription start sites and splicing at the C-terminus (Yang et al., 1998). Three isoforms contain the N-terminal transcriptional activation sequence (TAp63),

whereas the remaining three isoforms lack this sequence (ΔNP63). The ΔNP63 isoforms, which are the predominant isoforms expressed during tooth development (Laurikkala et al., 2006), were also the predominant transcripts expressed in LS8 cells (Fig. 1N), and thus are the likely transactivators responsible for *Perp* expression in dental epithelial cells.

PERP is localized between the ameloblasts and stratum intermedium cells

We examined the localization of PERP and DSP during amelogenesis in the continuously growing mouse incisor (for a review, see Thesleff et al., 2007), which enables visualization of ameloblasts at all stages of amelogenesis in a single sample. Sections at postnatal day (P) 7 were immunostained for PERP (Fig. 2F–I). For comparison, adjacent sections were stained with hematoxylin and eosin (H&E; Fig. 2A–E). PERP was localized to the ameloblast–SI interface as well as in the SI at all stages of amelogenesis: presecretory (Fig. 2F), secretory (Fig. 2G), transitional (Fig. 2H) and mature (Fig. 2I). DSP was also expressed
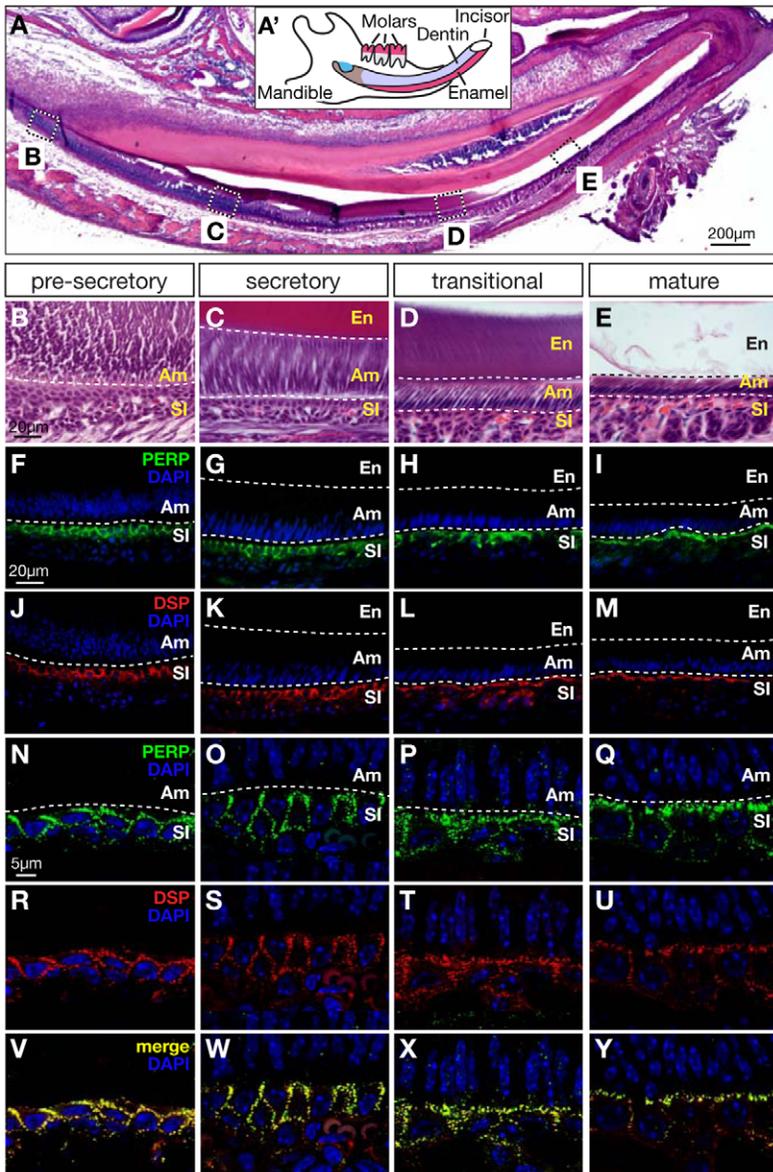

Fig. 2. PERP localization in developing incisors at P7.
(**A**) H&E staining of the lower incisor and mandible in sagittal section. (**A′**) Cartoon of the mandible. (**B–E**) H&E staining of the lower incisor. (**F–I**) PERP immunofluorescence staining at pre-secretory, secretory, transitional and mature stages. (**J–M**) DSP immunofluorescence staining during amelogenesis. (**N–Y**) High-magnification views of double immunofluorescence staining of PERP and DSP show colocalization at ameloblast–SI interface. En, enamel; Am, ameloblasts; SI, stratum intermedium.
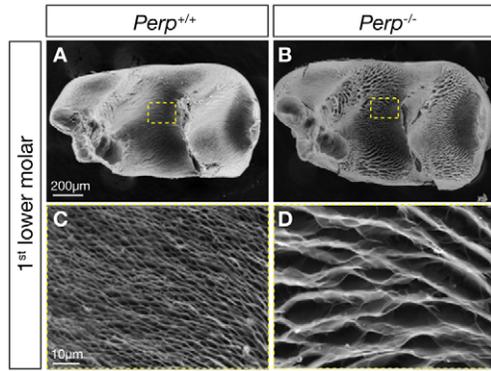
Fig. 3. SEM analysis of teeth at P2. (A,C) Low-magnification images of the enamel surface of the first lower molars from wild-type (*Perp*$^{+/+}$) and *Perp*-null (*Perp*$^{-/-}$) mice. **(B,D)** Higher-magnification images of the boxed areas.

in the ameloblast–SI interface and the SI (Fig. 2J–M). Higher magnification images of double immunofluorescence staining showed colocalization of PERP and DSP in the ameloblast–SI interface and the SI (Fig. 2N–Y).

PERP is required for formation of normal enamel

To examine the role of PERP in tooth development, developing first molars were isolated from wild-type and *Perp*-null mice at P2, the tissues surrounding the mineralized enamel and dentin were removed and the surfaces visualized by scanning electron microscopy (SEM; Fig. 3). Enamel formation was defective in upper and lower molars of *Perp*-null mice compared with that in wild-type littermates (Fig. 3). We detected differences in the architecture between enamel in wild-type and *Perp*-null mice, suggesting abnormalities in secretion of the enamel extracellular matrix and its subsequent mineralization. Interestingly, teeth from heterozygous mice displayed a range of phenotypes between those observed in wild-type and *Perp*-null specimens (supplementary material Fig. S2A–D).

In contrast to the enamel, there were no detectable differences by SEM analysis in the dentin of *Perp*-null specimens (supplementary material Fig. S2E–G). We also assayed *Perp* levels by qPCR in teeth from wild-type, *Perp*-heterozygous null and *Perp*-homozygous null mice (supplementary material Fig. S2H). *Perp* expression in the heterozygotes was approximately half the level of that in wild-type mice. Together with the range of phenotypes observed in the heterozygotes, these data suggest that

there is a threshold level for *Perp* expression of approximately 50%, below which abnormal amelogenesis occurs.

We next analyzed tooth sections from wild-type and *Perp*-null mice at P7 with H&E staining, and we observed dramatic defects in the enamel matrix, consistent with the SEM data. The dentin and pulp appeared normal, although the dentin matrix was thinner and the teeth appeared to be smaller in *Perp*-null mice at P7 (Fig. 4). In lower incisors (Fig. 4A–B′) and first upper molars (Fig. 4C–D′), the wild-type enamel matrix was uniform in appearance, whereas the matrix from *Perp*-null mice was irregular in staining and consisted of a mixture of dense and clear regions, suggesting a deficiency in matrix proteins and/or resorption. We next examined tooth sections from E16.5, P0 and P3 mice to determine the point at which the enamel phenotype was first detectable (supplementary material Fig. S3). There were no differences in the enamel matrix between wild-type and *Perp*-null mice at E16.5 and P0 (supplementary material Fig. S3A–H′). We first observed enamel defects in the lower incisors at P3 where there was less dense enamel matrix near the dentine surface–enamel junction (supplementary material Fig. S3J′).

Perp-null mice show a detachment of ameloblasts from the SI

The abnormal enamel matrix in *Perp*-null teeth led us to examine the ameloblasts in the mutants. The ameloblasts adhered tightly to the SI in the wild-type incisors (Fig. 5A,C), whereas incisors in *Perp*-null mice showed displacement and ectopic localization of ameloblasts between the ameloblast layer and enamel matrix at the transitional stage of amelogenesis (Fig. 5B). DAPI staining showed that the nuclei of these displaced cells were intact (Fig. 5D), and there was no evidence of pyknosis to indicate apoptosis or necrosis (data not shown). Moreover, we did not detect any differences in apoptosis by TUNEL staining or proliferation by PCNA staining in teeth from wild-type and mutant mice (data not shown). These displaced cells also expressed ameloblast-specific markers such as ameloblastin (AMBN; Fig. 5E,F) and amelogenin (AMEL; Fig. 5G,H), indicating that these cells are indeed ameloblasts that became detached from the underlying SI layer.

Perp-null mice have compromised desmosomes at the ameloblast–SI interface

Transmission electron microscopy (TEM) analyses of the developing incisor at P2 showed wider spaces between the secretory ameloblasts and the SI in *Perp*-null mice than in controls (Fig. 6A,B), consistent with the detachment of cells seen by histological
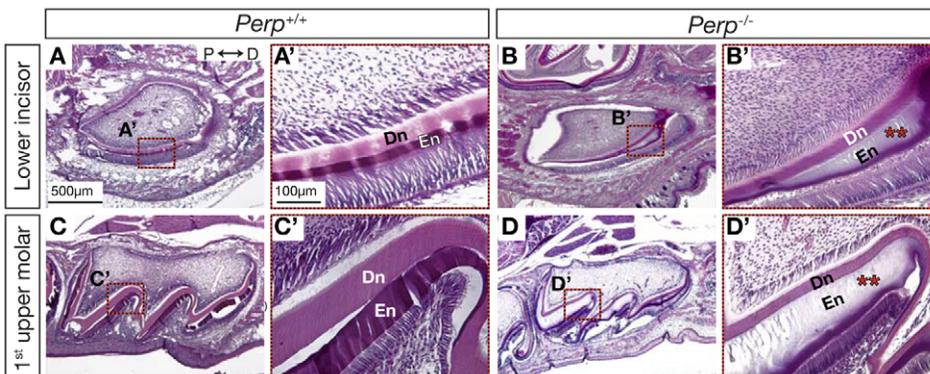

Fig. 4. H&E staining of developing mandibular incisors and maxillary molars in wild-type (*Perp*$^{+/+}$) and *Perp*-null (*Perp*$^{-/-}$) mice at P7 in sagittal sections. (A–D) Low-magnification images of the lower incisor and 1st upper molar. **(A′–D′)** Higher-magnification images of the boxed areas. Dentin (Dn) and enamel (En) are denoted by yellow and red arrowheads, respectively. Areas of defective enamel are denoted by red asterisks in the incisors and molars of *Perp*-null mice. P, proximal; D, distal.
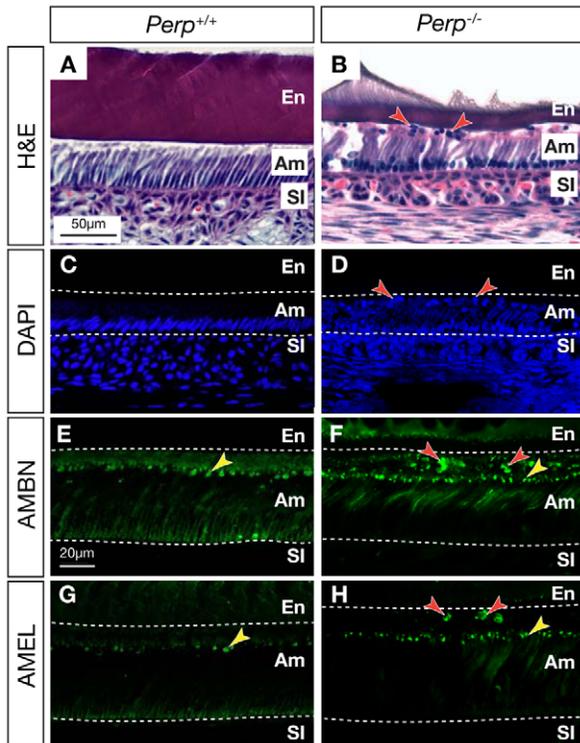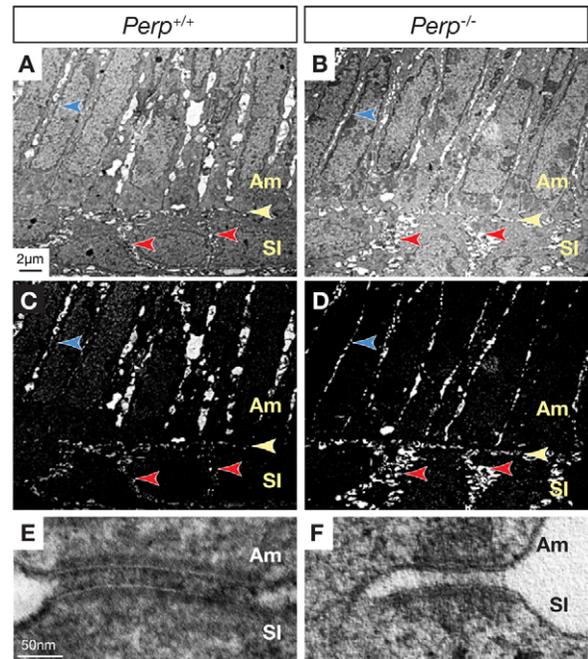
Fig. 5. Displacement of ameloblasts from the SI. (**A**,**B**) H&E staining of the transitional stage in sagittal sections of incisors at P7. Detached cells between ameloblasts and the enamel matrix in *Perp*-null mice are indicated (red arrowheads). (**C**,**D**) DAPI staining of adjacent sections shows the presence of the detached cells (red arrowheads). (**E–H**) Detached cells express ameloblast-specific proteins such as ameloblastin (AMBN, red arrowheads) and amelogenin (AMEL; red arrowheads). Matrix vesicles present in both wild-type and *Perp*-null teeth are indicated (yellow arrowheads). En, enamel; Am, ameloblasts; SI, stratum intermedium.

Fig. 6. Transmission electron microscope (TEM) analysis of desmosomes at the ameloblast-SI interface in wild-type (*Perp*$^{+/+}$) and *Perp*-null (*Perp*$^{-/-}$) mice at P2. (**A–D**) Native (A,B) and contrast-enhanced (C,D) TEM images show greater separation between the secretory ameloblasts and the SI (yellow arrowheads) and between the cells in the SI (red arrowheads), but not between ameloblasts (blue arrowheads), in *Perp*-null mice compared with the wild type. (**E,F**) Representative desmosomes from wild-type and *Perp*-null mice. (**G**) Reduced number and size of desmosomes at the ameloblast–SI interface in *Perp*-null mice compared with the wild type. Am, ameloblasts; SI, stratum intermedium. **P<0.01.

staining in older specimens at P7 (Fig. 5). Contrast-enhanced images illustrated wider spaces along the ameloblast–SI interface as well as between the cells of the SI, but we did not reproducibly detect larger separation between ameloblasts (Fig. 6C,D). Higher magnification images showed abnormal desmosomes with decreased electron density and reduced size in *Perp*-null mice compared with wild-type mice (Fig. 6E,F). There were significantly fewer and smaller desmosomes along the ameloblast–SI interface in mutant mice (Fig. 6G).

Microarray and qPCR analyses of teeth from wild-type versus *Perp*-null mice

To examine gene expression differences between wild-type and *Perp*-null mice in an unbiased fashion, we performed microarray analysis using total RNA isolated from epithelium of first lower molars of male mice at P0. We chose this time point because it precedes the earliest enamel defect we detected at P2. We observed a large number of changes in gene expression (supplementary material Fig. S4A). We analyzed the genes with a greater than twofold change and a *P*-value of <0.05 using Gene Ontology (GO) enrichment from two hand-curated databases (Ingenuity and Metacore), and identified molecular pathways and biological processes altered in mutant teeth. Ingenuity Pathway Analysis (IPA) of differentially expressed genes identified five molecular

functions significantly enriched in teeth at P0 (supplementary material Fig. S4B) with 'cell-to-cell signaling and interaction' as the top network (*P*=2.41E-11). The driving biological process of this network was cell adhesion, consisting of 287 differentially expressed genes (*P*=2.41E-11). To better define the function of these gene members we performed Metacore analysis and found different cell adhesion processes highly represented. The top processes included chemotaxis and cell–matrix interactions (supplementary material Fig. S4C; FDR<0.05).

Specific to enamel formation, we found changes in the expression of several genes known to be involved in amelogenesis, but interestingly, other genes involved in this process appeared to be unaffected (Fig. 7A). Using qPCR, we validated the microarray findings that *Ambn* (ameloblastin), *Enam* (enamelin), *Mmp20* (matrix metalloproteinase-20) and *Klk4* (kallikrein 4), as well as *Perp* itself, were downregulated in *Perp*-null mice (Fig. 7B). By contrast, *Amel* (amelogenin), *Tuft1* (tuftelin 1) and *Odam* (odontogenic ameloblast-associated or Apin) were not differentially expressed in *Perp* mutants (Fig. 7B). Little or no expression of
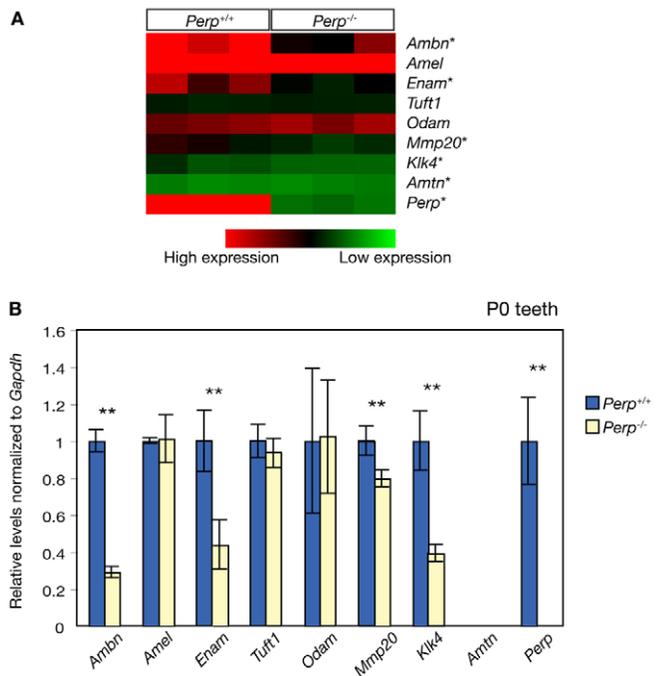
Fig. 7. Relative expression of genes involved in amelogenesis. (**A**) Heat map depiction of candidate genes involved in amelogenesis from the microarray comparison of first lower molars of wild-type and *Perp*-null mice at P0. Percentage expression changes relative to wild-type are displayed in brackets and any changes >1.75-fold are denoted with an asterisk (*). Red and green represent high and low expression, respectively. (**B**) qPCR analysis shows significant downregulation of *Ambn*, *Enam*, *Mmp20*, *Klk4* and *Perp* in teeth of *Perp*-null mice, whereas *Amel*, *Tuft1* and *Odam* are unaffected. No or little expression of *Amtn* is shown by microarray and qPCR analyses. *Ambn*, ameloblastin; *Amel*, amelogenin; *Enam*, enamelin; *Tuft1*, tuftelin 1; *Odam*, odontogenic ameloblast-associated (or Apin); *Mmp20*, matrix metalloproteinase 20, *Klk4*, kallikrein 4; *Amtn*, amelotin. **P<0.01.

Amtn (amelotin) was observed in P0 teeth, consistent with previous reports (Iwasaki et al., 2005). We also confirmed the downregulation of ameloblastin and unchanged expression of amelogenin in *Perp*-null male mice by immunofluorescence staining (supplementary material Fig. S5).

siRNA knockdown of PERP in LS8 ameloblast-derived cells

To test the effects of acute knockdown of PERP in ameloblast-derived cells, as opposed to development in the chronic absence of PERP in the *Perp*-null mice, we used siRNA technology in LS8 cells (Fig. 8 and supplementary material Fig. S6). We first tested whether PERP was present in LS8 cells and was successfully knocked down using siRNAs (Fig. 8A and supplementary material Fig. S6). The expression profiles of amelogenesis genes in scrambled versus PERP-knockdown cells were comparable with those observed in the teeth of wild-type versus *Perp*-null mice, indicating that LS8 cells responded to the absence of PERP similarly to dental epithelial cells in vivo (Fig. 8B). The exceptions were *Odam*, which showed little or no expression in LS8 cells and *Amel*, which was downregulated with the knockdown of PERP in vitro, but was not changed in teeth from the *Perp*-null mice. Thus, our in vitro studies confirm the in vivo regulation of genes involved in amelogenesis by PERP.
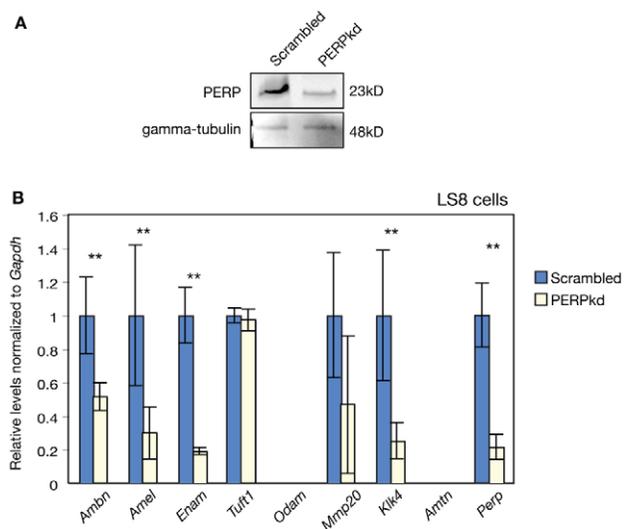

Fig. 8. Knockdown of PERP in LS8 cells using siRNA. (**A**) The knockdown of PERP with siRNA (PERPkd) relative to scrambled control was demonstrated by western blot analysis. (**B**) *Ambn*, *Amel*, *Enam*, *Klk4* and *Perp* were significantly downregulated in PERPkd LS8 cells. There was little or no expression of *Odam* and *Amtn*. qPCR results were normalized to *Gapdh* as an internal control and expression levels are relative to scrambled controls. **P<0.01.

Identification of additional PERP-regulated genes

From the microarray analysis, we next identified genes that were highly differentially expressed and not previously implicated in amelogenesis. From an initial selection of ten genes that showed greater than fourfold change between wild-type and mutants, we confirmed the differential expression of four genes by qPCR, namely *Dmkn* (dermokine), *Sost* (sclerostin), *Lama2* (laminin α2) and *Krt83* (keratin-83) (Fig. 9A). The remaining genes from the initial selection failed to show differential expression by qPCR, possibly because of the low levels of expression in teeth. We assayed for the expression of the four differentially expressed genes in LS8 cells with or without PERP knockdown (Fig. 9B). *Dkmn* and *Sost* were downregulated with in vitro PERP knockdown, whereas expression of *Lama2* and *Krt83* was unchanged.

Discussion

In this study, we found that PERP, which is necessary for the stable assembly and integrity of desmosomes, is required for the attachment of ameloblasts to the adjacent SI layer during amelogenesis. In *Perp*-null mice, we observed separation at the ameloblast–SI interface as well as discontinuities between SI cells, and these cellular changes were associated with dramatic enamel defects. The number and size of the desmosomes along the ameloblast–SI interface were decreased and this was reflected by the separation and detachment of ameloblasts from the SI layer. Several genes were differentially expressed between wild-type and *Perp*-null mice during amelogenesis, and we confirmed the genes identified from teeth in vivo against an in vitro cell culture model.

Perp and *Tp63*

In the developing tooth at embryonic stages, PERP and DSP are colocalized in the SI and SR with some staining in the IEE, a layer of epithelial cells from which ameloblasts are derived. During amelogenesis, PERP and DSP are colocalized at the ameloblast–SI
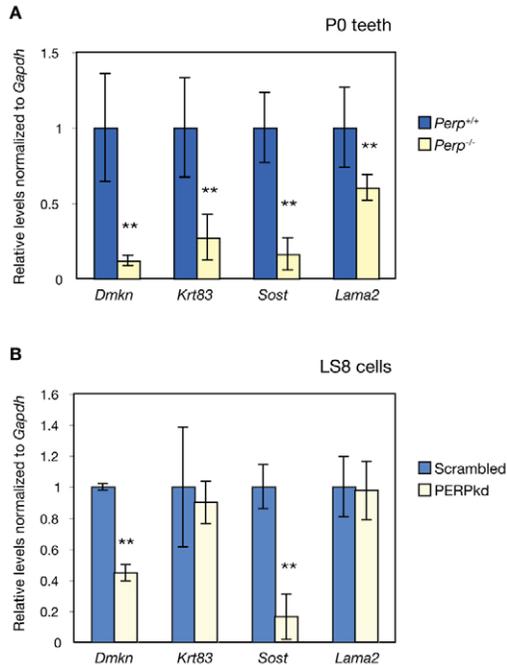
Fig. 9. Identification of additional genes regulated by PERP. (A) qPCR was used to confirm differentially expressed genes determined by microarray analysis. *Dmkn*, *Krt83*, *Sost* and *Lama2* were significantly downregulated in teeth of *Perp*-null mice. **(B)** *Dmkn* and *Sost* were also downregulated in LS8 cells with PERP knockdown (PERPkd), whereas *Krt83* and *Lama2* were unchanged. qPCR results were normalized to *Gapdh* as an internal control and expression levels are relative to wild-type or scrambled controls. *Dmkn*, dermokine; *Krt83*, keratin-83, *Sost*, sclerostin; *Lama2*, laminin α2. **P<0.01.

interface and the SI, and this localization profile overlaps with that of P63.

The overlapping localization profiles of P63 and PERP in developing teeth are consistent with our in vitro data that expression of *Perp* is regulated by P63. P63 is a member of the P53 protein family that regulates stratified epithelial development as well as craniofacial and limb morphogenesis (Mills et al., 1999; Senoo et al., 2007; Yang et al., 1999). In mice lacking *Tp63*, all ectodermal organs including teeth fail to develop (Laurikkala et al., 2006). We found that *Perp* is a downstream target of P63 in amelogenesis, as shown by activity of the *Perp* reporter in ameloblast-derived cells in vitro. We also showed that the ΔNP63 isoforms, the main isoforms of P63 expressed during development (Laurikkala et al., 2006; Truong et al., 2006), are the likely regulators of *Perp* expression in dental epithelia. The low but detectable activity of the mutated *Perp* reporter indicates that other activators and/or additional P63-responsive elements are also involved in regulation of *Perp*. In light of the observation that genes such as *Bmp7* (bone morphogenetic protein-7), *Jag1* (jagged-1), *Notch1* (notch gene homolog-1) and *Fgfr2* (fibroblast growth factor receptor-2) lie downstream of *Tp63* (Laurikkala et al., 2006), it is possible that the proteins encoded by these genes also regulate *Perp* expression.

PERP is required for ameloblast–SI attachment and proper desmosomes

A central finding in our study of teeth in *Perp*-null mice was the separation and ectopic displacement of the ameloblasts from the SI at the secretory and transitional stages of amelogenesis. This

observation is consistent with the reduced number and size of desmosomes at the ameloblast–SI interface in the teeth of *Perp*-null mice, and it supports a role for the ameloblast–SI interface during amelogenesis. Notably, the detachment of ameloblasts did not appear to affect either cell survival or gene expression (i.e. *Ambn* and *Amel* expression).

The reduced size of desmosomes in *Perp*-null teeth contrasts with the slightly increased desmosome size in the skin of *Perp*-null mice (Ihrie et al., 2005). The reasons for this difference could include tissue- or cell-specific effects of PERP and secondary effects due to other adhesion proteins, and this issue will require further study.

A role for the ameloblast–SI interface was previously highlighted in a study involving nectin-1 (Barron et al., 2008). Although nectin-1 is known to be important in both adherens and tight junctions (Fukuhara et al., 2002a; Fukuhara et al., 2002b), deletion of nectin-1 also led to changes in desmosome number and size, consistent with separation of the ameloblast–SI interface. However, there are several important differences between the nectin-1 mutants and the *Perp*-null mice: (1) separation of the ameloblast–SI interface occurred at the mature, but not secretory stage of amelogenesis in *nectin-1* mutants; (2) the displacement and localization of ameloblasts between the ameloblast layer and enamel matrix did not occur in nectin-1 mutants; (3) unlike in the *Perp*-null mice, where all teeth showed enamel defects, only the incisors showed enamel defects in nectin-1 mutants; and (4) in nectin-1 mutants, separation between ameloblasts appears to occur before separation between the ameloblast and SI layer (Barron et al., 2008). The absence of an enamel phenotype in nectin-1 mutant molars is particularly surprising considering that desmosomal proteins are highly expressed in all teeth and might be involved in the morphogenesis and early positioning of molars (Cam et al., 2002; Fausser et al., 1998; Kieffer-Combeau et al., 2001; Lesot et al., 2002). Because nectin-1 is not localized to desmosomes, it appears likely that the desmosomal abnormalities in nectin-1-knockout mice are indirect results of defects in the adherens and tight junctions. Indeed, there are several reports demonstrating that abnormalities in the adherens junctions can affect desmosomes (Chen et al., 2002; Hatzfeld et al., 2003; Lewis et al., 1997). By contrast, the role of PERP has been demonstrated to be specific to desmosome integrity and does not appear to affect adherens junctions or tight junctions (Ihrie et al., 2005); additionally, we did not detect any changes in expression of genes encoding E-cadherin or claudin in our array experiments. Therefore, the *Perp*-null mice provide the first potential model for the study of desmosomes at the ameloblast–SI interface.

PERP and the regulation of gene expression

We used microarray technology to identify differentially expressed genes in teeth from wild-type and *Perp*-null mice. Bioinformatic analysis revealed 'cell-to-cell signaling and interaction' as the top molecular and cellular function to be highly enriched in mutant mice. However, none of the desmosome components (i.e. genes encoding cadherin, armadillo and plakin) appeared to be differentially expressed in mutants (data not shown). Therefore, the reduction in desmosome number and size that we detected by TEM in *Perp* mutants is probably due to the post-transcriptional regulation of desmosomal component genes. Specific to enamel formation, we found that several known regulators of amelogenesis such as *Ambn*, *Enam*, *Mmp20* and *Klk4* were downregulated in *Perp*-null mice, whereas others such as *Amel*, *Tuft1* and *Odam* were unchanged. Our in vitro experiments demonstrated that *Ambn*,

Enam and *Klk4* were all significantly downregulated with the knockdown of PERP. *Amel* was also downregulated with PERP knockdown despite our observation that expression levels were unchanged in teeth. This might be caused by the artificial in vitro environment, or it might be attributable to sex differences, because the teeth used in the microarray analysis and qPCR confirmations were from male mice, whereas LS8 cells were derived from female mice (data not shown); sex-dependent regulation of *Amel* has been shown previously (Chapman et al., 1991; Hu et al., 2007; Salido et al., 1992). Therefore, *Ambn*, *Enam*, *Klk4* and *Amel* (in female mice only) were confirmed to be regulated by PERP in vitro.

The downregulation of *Ambn*, *Amel* and *Enam* at the secretory stage of amelogenesis in *Perp*-null mice at P0 is consistent with defects in matrix deposition and mineralization that were detected by SEM analysis at P2. In fact, *Ambn*, *Amel* and *Enam* comprise 90–99% of the enamel matrix (Hu et al., 2007). However, the downregulation of *Mmp20* and *Klk4* in *Perp*-null mice also suggests that the resorption of the matrix is defective. MMP20 and KLK4 are proteins that are predominant at the transitional and mature stages of amelogenesis when the matrix is resorbed and almost completely replaced with mineral (Hu et al., 2007; Stephanopoulos et al., 2005). We detected the detachment and ectopic displacement of ameloblasts from the SI at the transitional stage. Thus, *Perp* appears to be important at both the secretory and transitional stages of amelogenesis. Further study is required to understand why *Tuft1* and *Odam*, genes that are predominantly expressed during the secretory and transitional stages, respectively, were unaffected.

In addition to the identification of differentially expressed candidate genes during amelogenesis, four genes of unknown function in amelogenesis (*Dmkn*, *Sost*, *Krt83* and *Lama2*) were discovered to be differentially expressed in teeth from *Perp* mutants compared with those from wild-type mice. In vitro, Dmkn and *Sost* had decreased expression after PERP knockdown in LS8 cells, whereas *Krt83* and *Lama2* did not. This highlights the differences between in vivo and in vitro environments and suggests that the differential expression of *Krt83* and *Lama2* requires factors additional to PERP.

Dmkn encodes a secreted protein of unknown function that is highly expressed in the spinous and granular layers of stratified epithelia (Matsui et al., 2004) but is also expressed in the gut, lung, breast, liver and pancreas (Naso et al., 2007). The wide expression profile of *Dmkn* is reminiscent of that for *Perp*, which is expressed in stratified epithelia as well as in the heart, forestomach, submandibular gland and thymus (Ihrie et al., 2005).

Sost encodes a secreted protein that antagonizes BMP and WNT activity (ten Dijke et al., 2008). Although there are reports regarding dental abnormalities such as anodontia (missing teeth) and unerupted teeth in patients with *Sost* mutations (Stephen et al., 2001), there have been no detailed dental studies in these patients. It is interesting that ameloblasts appear to express *Sost*, a known inhibitor of bone resorption (ten Dijke et al., 2008), and that proteins released during amelogenesis might regulate the eruption of teeth.

Krt83 belongs to the large family of hair keratins that are expressed in ectodermal structures such as hairs, nails and claws (Langbein et al., 2001). Mutations in *Krt83* have been associated with monilethrix, an autosomal hair disorder that can cause scarring alopecia (Carreras, 1996; van Steensel et al., 2005), and the hairless phenotype of the Hirosaki hairless rat (Nanashima et al., 2008). Hair keratins, and in particular *Krt83*, have yet to be studied in teeth.

Lama2 encodes a component of the hemidesmosomes that normally bind the ameloblast layer to the enamel matrix and are present at the ameloblast–enamel interface in the mature ameloblasts (Yuasa et al., 2004). Presumably, the presence of detached ameloblasts between the ameloblast layer and enamel matrix observed in *Perp*-null mice either requires or causes a compromise in the hemidesmosomes. This hypothesis is supported by the identification of 'cell-matrix interactions' as one of the top molecular and cellular processes to be enriched in *Perp* mutants.

PERP and amelogenesis imperfecta

Amelogenesis imperfecta (AI) is a group of inherited disorders of enamel (Fleischmannova et al., 2008; Hu et al., 2007; Stephanopoulos et al., 2005). To date, at least six genes are known to be involved in human AI: *AMEL*, *AMBN*, *ENAM*, *DLX3*, *MMP20* and *KLK4*. Defects in *AMEL*, *AMBN* and *ENAM* affect the secretory stages of amelogenesis (Hu et al., 2007; Stephanopoulos et al., 2005). Mutations in *DLX3* lead to enamel hypoplasia and the enlargement of the pulp (Dong et al., 2005). *MMP20* and *KLK4* are required for resorption of the enamel matrix and proper completion of mineralization (Bourd-Boittin et al., 2005; Hu et al., 2002; Iwata et al., 2007; Yamakoshi et al., 2006). In *Perp*-null mice and in cells with PERP knockdown, several genes associated with human AI (Hu et al., 2007; Stephanopoulos et al., 2005) were differentially expressed, namely *Ambn*, *Amel*, *Enam*, *Mmp20* and *Klk4*. These data suggest that *Perp*, and perhaps other genes encoding desmosomal components, are candidate genes for human AI.

Our findings thus point to a model in which PERP is essential for amelogenesis involving cell–cell adhesion, in part, through desmosome-mediated interactions between the ameloblasts and the SI. Our data indicate that *Perp* expression in teeth is directly regulated by P63, which is upstream of other genes that might also affect tooth development, including *Bmp7*, *Jag1*, *Notch1* and *Fgfr2* (Laurikkala et al., 2006). In turn, PERP is necessary for the proper number and size of desmosomes at the ameloblast–SI interface, without which the ameloblasts detach from the SI layer. Thus, PERP is crucial for enamel formation through its effects on cell–cell adhesion, and loss of PERP leads to both abnormal adhesion and misregulation of gene expression.

Materials and Methods

Animals
The generation, genotyping and initial analysis of *Perp*-null mice have been described earlier (Ihrie et al., 2005). Mice were mated overnight, and the day of formation of a vaginal plug was taken as embryonic day 0.5.

Histology
Embryonic and postnatal tissues for histology and immunostaining were fixed overnight in 4% paraformaldehyde or Bouin's fixative at 4°C, dehydrated, embedded in paraffin wax, and serially sectioned at 7 µm. Heads from E16.5 and E18.5 embryos and postnatal animals were demineralized in 0.5 M EDTA for 3–7 days. Histological sections were stained with hematoxylin and eosin (H&E).

Immunohistochemistry
Immunohistochemistry was performed according to standard protocols. Primary antibodies used were as follows: anti-P63 (1:200; Abcam), anti-PERP (1:100; Abcam), anti-desmoplakin (DSP; 1:50; AbD Serotec), anti-amelogenin (AMEL; 1:200; Abcam) and anti-ameloblastin (AMBN; 1:200; Abcam). Goat anti-rabbit or mouse Alexa Fluor 488 or Alexa Fluor 555 secondary antibodies were used (1:250; Invitrogen). For double immunofluorescence staining, slides were heat-treated in Trilogy (Cell Marque) for 20 minutes and cooled at room temperature for 20 minutes after deparaffinization and rehydration.

Cell culture
LS8 cells (Chen et al., 1992; Xu et al., 2006) were plated with 10% FBS (HyClone Sera; UCSF), DMEM High Glucose (DME-H21; UCSF) and penicillin-streptomycin. For transient transfections, LS8 cells were cultured in medium without penicillin-streptomycin, and for cell adhesion assays, 1 mM $CaCl_2$ was added. Cells were grown in a humidified air and CO_2 (19:1) mixture at 37°C, and medium was changed every 2–3 days.

Transient transfections
LS8 cells were plated onto 24-well plates at a density of 50,000 cells/well and incubated overnight. One µl of Lipofectamine 2000 reagent (Invitrogen) was used according to the manufacturer's protocol. For promoter assays, 1 µg of PerpLuc-wt, PerpLuc-mut (Reczek et al., 2003), or pGL3-basic vector was co-transfected with 0.1 µg of *Renilla* plasmid (Promega). For RNA interference experiments, 4 µmoles of individual siRNA1 (GUGGGAAGAAGCCGUGUUA), siRNA2 (GCUUAGAACCAGCGUAGAC), siRNA3 (UCGCUUUGGUGGAGGUGUU), siRNA4 (GCAUCGUUUGUGAGAAUUU), siRNA 1+2, or pooled siRNA (i.e. 1+2+3+4) specific for the knockdown of PERP (ON-TARGETplus SMARTpool, Dharmacon), GAPDH (Ambion), or scrambled control (Ambion) were transfected and the cells harvested after 24 hours.

Luciferase assays
Luciferase assays were performed using the Dual-Luciferase Reporter Assay System (Promega) and the Synergy 2 chemiluminescence microplate reader (Biotek).

Cell lysate and RNA isolation
Cell lysates and total RNA were isolated using the RNeasy kit (Qiagen). DNA was removed in-column with RNase-free DNase (Qiagen).

PCR and qPCR
All PCR reactions were performed using the GoTaq PCR Master Mix (Promega) in a Mastercycler (Eppendorf). All qPCR reactions were performed using the GoTaq qPCR Master Mix (Promega) in a Mastercycler Realplex (Eppendorf). Primers specific for the various P63 isoforms have been previously described (Truong et al., 2006). All other primers were designed using PerlPrimer3 software (Rozen and Skaletsky, 2000), and sequences are available upon request. qPCR conditions were as follows: 95°C, 2 minutes; 40 cycles at 95°C, 15 seconds; 58°C, 15 seconds; 68°C, 20 seconds; followed by a melting curve gradient. Expression levels of the genes of interest were normalized to levels of *Gapdh* and are presented as relative levels to control or wild type.

Scanning electron microscopy
First molars were dissected from P2 mice and placed in water for 1 hour. Cells and tissues were removed manually from the dentin and enamel, rinsed in bleach, and stored in 70% ethanol. The mineralized dentin and enamel were incubated in 1% osmium tetraoxide solution in 70% ethanol for 1 hour followed by three changes in 70% ethanol. The samples were dehydrated through an alcohol gradient series and then air-dried for 15–30 minutes. Samples were then mounted on metal stubs and visualized by a scanning electron microscope (Hitachi TM-1000).

Transmission electron microscopy
Heads were dissected from P2 mice, cut sagittally along the midline, and immediately fixed for 1 hour at room temperature and overnight at 4°C in Karnovsky fixative (2% glutaraldehyde and 3% paraformaldehyde in 0.1 M cacodylate buffer at pH 7.4). Samples were washed in cacodylate buffer and then demineralized for 4 days in PBS containing 12.5% EDTA and 0.8% glutaraldehyde at 4°C with rocking and daily solution change. Following demineralization, each of the half heads was cut through the oral cavity to separate the hemi-mandible from the maxilla. Hemi-mandibles were post-fixed for 2 hours in PBS containing 1% osmium tetraoxide, 0.5% potassium dichromate, and 0.5% potassium ferrocyanide. Samples were washed in PBS and stained in 2% uranyl acetate in water for 2 hours in the dark on a rocking table. Following staining, samples were washed with water, dehydrated in an ethanol gradient followed by propylene oxide and embedded in Epon resin. Each of the mandibular incisors was cut perpendicular to the midline at approximately the level of the first molar and embedded in resin for 48 hours. Sections (~80 nm thick) were cut using a Leica Ultracut ultramicrotome, transferred to formvar-coated Cu grids, and post-stained with Reynold's lead citrate and 2% uranyl acetate in 50% ethanol for 5 and 15 minutes, respectively. Grids were examined on an FEI Tecnai 20 TEM operating at 100 kV and imaged on an AMT 16000-S CCD camera. Images are presented either in the native state or after contrast enhancement using Photoshop (Adobe).

Microscopy
Fluorescent and bright field images were taken using a Leica DM5000B with a Leica DFC500 camera. For confocal images, a Leica SP5 Upright Confocal was used.

Microarray and differential expression analysis
First lower molars from wild-type and *Perp*-null mice at P0 were dissected and RNA isolated as described above. Probe labeling and array hybridizations were performed according to standard protocols from the UCSF Shared Microarray Core Facilities and Agilent Technologies (www.arrays.ucsf.edu and www.agilent.com). Total RNA quality was assessed using a Pico Chip on an Agilent 2100 Bioanalyzer (Agilent Technologies, Palo Alto, CA). RNA was amplified and labeled with Cy3–CTP using the Agilent low RNA input fluorescent linear amplification kits following the manufacturer's protocol (Agilent). Labeled cRNA was assessed using the Nandrop ND-100 (Nanodrop Technologies, Wilmington DE), and equal amounts of Cy3-labeled target were hybridized to whole mouse genome 4×44K Ink-jet arrays

(Agilent). Hybridizations were performed for 14 hours, according to the manufacturer's protocol. Arrays were scanned using a microarray scanner and raw signal intensities were extracted with Feature Extraction v10.3 software (Agilent).

Raw log intensities were normalized using the *quantile* normalization method (Bolstad et al., 2003). No background subtraction was performed, and the median feature pixel intensity was used as the raw signal before normalization. A two-way ANOVA model and specific contrasts were formulated to examine comparisons between treatments (wild-type versus *Perp*-null). Moderated t-statistic, B statistic, false discovery rate, and *P*-value for each gene were obtained. Adjusted *P*-values were produced by the method proposed by Holm (Holm, 1979). All procedures were carried out using functions in the 'R' package *limma in Bioconductor* (Gentleman et al., 2004; Smyth, 2004). The data discussed in this publication have been deposited in NCBI's Gene Expression Omnibus (Edgar et al., 2002) and are accessible through GEO Series accession number GSE26796 (http://www.ncbi.nlm.nih.gov/geo/query/acc.cgi?acc=GSE26796).

Bioinformatic analysis
Differential expression analysis was performed using the BrB-Array tool with standard parameters. The median over the entire array was used as reference for the normalization and a *P*-value of 0.01 used for the log intensity variation. Gene Ontology (GO) enrichment was performed using Ingenuity Pathway Analysis (IPA, Ingenuity® Systems, www.ingenuity.com) and Metacore (www.genego.com/metacore.php).

Western blot hybridization
Cell lysates were collected from siRNA-treated LS8 cells as described above. Protein levels were determined using the BCA Protein Assay kit (Thermo Scientific) according to the manufacturer's protocol. Two µg of protein was loaded onto a NuPAGE Novex 4–12% Bis-Tris gel (Invitrogen) and western blot hybridization was performed using standard protocols. Anti-γ-tubulin (1:1000, Sigma) was used as a protein loading control.

Statistical analysis
All experiments were performed independently at least three times in triplicate, and if applicable, presented as mean ± s.d. Except for the microarray analysis, Student's *t*-test was used to determine *P*-values and *P*<0.01 was deemed to be significant.

Supplementary material available online at
http://jcs.biologists.org/cgi/content/full/124/5/745/DC1

References

Attardi, L. D., Reczek, E. E., Cosmas, C., Demicco, E. G., McCurrach, M. E., Lowe, S. W. and Jacks, T. (2000). PERP, an apoptosis-associated target of p53, is a novel member of the PMP-22/gas3 family. *Genes Dev.* **14**, 704-718.

Barron, M. J., Brookes, S. J., Draper, C. E., Garrod, D., Kirkham, J., Shore, R. C. and Dixon, M. J. (2008). The cell adhesion molecule nectin-1 is critical for normal enamel formation in mice. *Hum. Mol. Genet.* **17**, 3509-3520.

Bolstad, B. M., Irizarry, R. A., Astrand, M. and Speed, T. P. (2003). A comparison of normalization methods for high density oligonucleotide array data based on variance and bias. *Bioinformatics* **19**, 185-193.

Bourd-Boittin, K., Fridman, R., Fanchon, S., Septier, D., Goldberg, M. and Menashi, S. (2005). Matrix metalloproteinase inhibition impairs the processing, formation and mineralization of dental tissues during mouse molar development. *Exp. Cell Res.* **304**, 493-505.

Cam, Y., Fausser, J. L., Vonesch, J. L., Peterkova, R., Peterka, M., Halaskova, M. and Lesot, H. (2002). Asymmetrical morphogenesis and medio-lateral positioning of molars during mouse development. *Eur. J. Oral Sci.* **110**, 35-43.

Carreras, D. (1996). Monilethrix: a review and case report. *Pediatr. Dent.* **18**, 331-333.

Casasco, M., Icaro Cornaglia, A., Riva, F., Calligaro, A. and Casasco, A. (2006). Expression of p63 transcription factor in ectoderm-derived oral tissues. *Ital. J. Anat. Embryol.* **111**, 125-131.

Chapman, V. M., Keitz, B. T., Disteche, C. M., Lau, E. C. and Snead, M. L. (1991). Linkage of amelogenin (Amel) to the distal portion of the mouse X chromosome. *Genomics* **10**, 23-28.

Chen, L. S., Couwenhoven, R. I., Hsu, D., Luo, W. and Snead, M. L. (1992). Maintenance of amelogenin gene expression by transformed epithelial cells of mouse enamel organ. *Arch. Oral Biol.* **37**, 771-778.

Chen, X., Bonne, S., Hatzfeld, M., van Roy, F. and Green, K. J. (2002). Protein binding and functional characterization of plakophilin 2. Evidence for its diverse roles in desmosomes and beta -catenin signaling. *J. Biol. Chem.* **277**, 10512-10522.

Dhamija, S., Liu, Y., Yamada, Y., Snead, M. L. and Krebsbach, P. H. (1999). Cloning and characterization of the murine ameloblastin promoter. *J. Biol. Chem.* **274**, 20738-20743.

Dong, J., Amor, D., Aldred, M. J., Gu, T., Escamilla, M. and MacDougall, M. (2005). DLX3 mutation associated with autosomal dominant amelogenesis imperfecta with taurodontism. *Am. J. Med. Genet.* **133A**, 138-141.

Edgar, R., Domrachev, M. and Lash, A. E. (2002). Gene Expression Omnibus: NCBI gene expression and hybridization array data repository. *Nucleic Acids Res.* **30**, 207-210.

Fausser, J. L., Schlepp, O., Aberdam, D., Meneguzzi, G., Ruch, J. V. and Lesot, H. (1998). Localization of antigens associated with adherens junctions, desmosomes, and hemidesmosomes during murine molar morphogenesis. *Differentiation* **63**, 1-11.

Fleischmannova, J., Matalova, E., Tucker, A. S. and Sharpe, P. T. (2008). Mouse models of tooth abnormalities. *Eur. J. Oral Sci.* **116**, 1-10.

Franke, W. W. (2009). Discovering the molecular components of intercellular junctions-a historical view. *Cold Spring Harb. Perspect. Biol.* **1**, a003061.

Freire-Maia, N. (1971). Ectodermal dysplasias. *Hum. Hered.* **21**, 309-312.

Fukuhara, A., Irie, K., Nakanishi, H., Takekuni, K., Kawakatsu, T., Ikeda, W., Yamada, A., Katata, T., Honda, T., Sato, T. et al. (2002a). Involvement of nectin in the localization of junctional adhesion molecule at tight junctions. *Oncogene* **21**, 7642-7655.

Fukuhara, A., Irie, K., Yamada, A., Katata, T., Honda, T., Shimizu, K., Nakanishi, H. and Takai, Y. (2002b). Role of nectin in organization of tight junctions in epithelial cells. *Genes Cells* **7**, 1059-1072.

Garrod, D. and Chidgey, M. (2008). Desmosome structure, composition and function. *Biochim. Biophys. Acta* **1778**, 572-587.

Gentleman, R. C., Carey, V. J., Bates, D. M., Bolstad, B., Dettling, M., Dudoit, S., Ellis, B., Gautier, L., Ge, Y., Gentry, J. et al. (2004). Bioconductor: open software development for computational biology and bioinformatics. *Genome Biol.* **5**, R80.

Green, K. J. and Simpson, C. L. (2007). Desmosomes: new perspectives on a classic. *J. Invest. Dermatol.* **127**, 2499-2515.

Hatzfeld, M., Green, K. J. and Sauter, H. (2003). Targeting of p0071 to desmosomes and adherens junctions is mediated by different protein domains. *J. Cell Sci.* **116**, 1219-1233.

Hay, M. F. (1961). The development in vivo and in vitro of the lower incisor and molars of the mouse. *Arch. Oral Biol.* **3**, 86-109.

Holm, S. (1979). A simple sequentially rejective multiple test procedure. *Scand. Stat. Theory Appl.* **6**, 65-70.

Hu, J. C., Sun, X., Zhang, C., Liu, S., Bartlett, J. D. and Simmer, J. P. (2002). Enamelysin and kallikrein-4 mRNA expression in developing mouse molars. *Eur. J. Oral Sci.* **110**, 307-315.

Hu, J. C., Chun, Y. H., Al Hazzazzi, T. and Simmer, J. P. (2007). Enamel formation and amelogenesis imperfecta. *Cells Tissues Organs* **186**, 78-85.

Huang, Z., Sargeant, T. D., Hulvat, J. F., Mata, A., Bringas, P., Jr, Koh, C. Y., Stupp, S. I. and Snead, M. L. (2008). Bioactive nanofibers instruct cells to proliferate and differentiate during enamel regeneration. *J. Bone Miner. Res.* **23**, 1995-2006.

Ihrie, R. A., Reczek, E., Horner, J. S., Khachatrian, L., Sage, J., Jacks, T. and Attardi, L. D. (2003). Perp is a mediator of p53-dependent apoptosis in diverse cell types. *Curr. Biol.* **13**, 1985-1990.

Ihrie, R. A., Marques, M. R., Nguyen, B. T., Horner, J. S., Papazoglu, C., Bronson, R. T., Mills, A. A. and Attardi, L. D. (2005). Perp is a p63-regulated gene essential for epithelial integrity. *Cell* **120**, 843-856.

Ihrie, R. A., Bronson, R. T. and Attardi, L. D. (2006). Adult mice lacking the p53/p63 target gene Perp are not predisposed to spontaneous tumorigenesis but display features of ectodermal dysplasia syndromes. *Cell Death Differ.* **13**, 1614-1618.

Iwasaki, K., Bajenova, E., Somogyi-Ganss, E., Miller, M., Nguyen, V., Nourkeyhani, H., Gao, Y., Wendel, M. and Ganss, B. (2005). Amelotin – a novel secreted, ameloblast-specific protein. *J. Dent. Res.* **84**, 1127-1132.

Iwata, T., Yamakoshi, Y., Hu, J. C., Ishikawa, I., Bartlett, J. D., Krebsbach, P. H. and Simmer, J. P. (2007). Processing of ameloblastin by MMP-20. *J. Dent. Res.* **86**, 153-157.

Jamora, C. and Fuchs, E. (2002). Intercellular adhesion, signalling and the cytoskeleton. *Nat. Cell Biol.* **4**, E101-E108.

Kieffer-Combeau, S., Meyer, J. M. and Lesot, H. (2001). Cell-matrix interactions and cell-cell junctions during epithelial histo-morphogenesis in the developing mouse incisor. *Int. J. Dev. Biol.* **45**, 733-742.

Langbein, L., Rogers, M. A., Winter, H., Praetzel, S. and Schweizer, J. (2001). The catalog of human hair keratins. II. Expression of the six type II members in the hair follicle and the combined catalog of human type I and II keratins. *J. Biol. Chem.* **276**, 35123-35132.

Laurikkala, J., Mikkola, M. L., James, M., Tummers, M., Mills, A. A. and Thesleff, I. (2006). p63 regulates multiple signalling pathways required for ectodermal organogenesis and differentiation. *Development* **133**, 1553-1563.

Lesot, H., Kieffer-Combeau, S., Fausser, J. L., Meyer, J. M., Perrin-Schmitt, F., Peterkova, R., Peterka, M. and Ruch, J. V. (2002). Cell-cell and cell-matrix interactions during initial enamel organ histomorphogenesis in the mouse. *Connect. Tissue Res.* **43**, 191-200.

Lewis, J. E., Wahl, J. K., 3rd, Sass, K. M., Jensen, P. J., Johnson, K. R. and Wheelock, M. J. (1997). Cross-talk between adherens junctions and desmosomes depends on plakoglobin. *J. Cell Biol.* **136**, 919-934.

MacDougall, M., Simmons, D., Dodds, A., Knight, C., Luan, X., Zeichner-David, M., Zhang, C., Ryu, O. H., Qian, Q., Simmer, J. P. et al. (1998). Cloning, characterization, and tissue expression pattern of mouse tuftelin cDNA. *J. Dent. Res.* **77**, 1970-1978.

Matsui, T., Hayashi-Kisumi, F., Kinoshita, Y., Katahira, S., Morita, K., Miyachi, Y., Ono, Y., Imai, T., Tanigawa, Y., Komiya, T. et al. (2004). Identification of novel keratinocyte-secreted peptides dermokine-alpha/-beta and a new stratified epithelium-secreted protein gene complex on human chromosome 19q13.1. *Genomics* **84**, 384-397.

Mills, A. A., Zheng, B., Wang, X. J., Vogel, H., Roop, D. and Bradley, A. (1999). p63 is a p53 homologue required for limb and epidermal morphogenesis. *Nature* **398**, 708-713.

Moffatt, P., Smith, C. E., St-Arnaud, R., Simmons, D., Wright, J. T. and Nanci, A. (2006). Cloning of rat amelotin and localization of the protein to the basal lamina of maturation stage ameloblasts and junctional epithelium. *Biochem. J.* **399**, 37-46.

Moffatt, P., Smith, C. E., St-Arnaud, R. and Nanci, A. (2008). Characterization of Apin, a secreted protein highly expressed in tooth-associated epithelia. *J. Cell. Biochem.* **103**, 941-956.

Nanashima, N., Akita, M., Yamada, T., Shimizu, T., Nakano, H., Fan, Y. and Tsuchida, S. (2008). The hairless phenotype of the Hirosaki hairless rat is due to the deletion of an 80-kb genomic DNA containing five basic keratin genes. *J. Biol. Chem.* **283**, 16868-16875.

Naso, M. F., Liang, B., Huang, C. C., Song, X. Y., Shahied-Arruda, L., Belkowski, S. M., D'Andrea, M. R., Polkovitch, D. A., Lawrence, D. R., Griswold, D. E. et al. (2007). Dermokine: an extensively differentially spliced gene expressed in epithelial cells. *J. Invest. Dermatol.* **127**, 1622-1631.

Owen, G. R. and Stokes, D. L. (2010). Exploring the nature of desmosomal cadherin associations in 3D. *Dermatol. Res. Pract.* **2010**, 930401.

Reczek, E. E., Flores, E. R., Tsay, A. S., Attardi, L. D. and Jacks, T. (2003). Multiple response elements and differential p53 binding control Perp expression during apoptosis. *Mol. Cancer Res.* **1**, 1048-1057.

Rozen, S. and Skaletsky, H. (2000). Primer3 on the WWW for general users and for biologist programmers. In *Bioinformatics Methods and Protocols: Methods in Molecular Biology* (ed. S. Krawetz and S. Misener), pp. 365-386. Totowa, NJ: Humana Press.

Rufini, A., Weil, M., McKeon, F., Barlattani, A., Melino, G. and Candi, E. (2006). p63 protein is essential for the embryonic development of vibrissae and teeth. *Biochem. Biophys. Res. Commun.* **340**, 737-741.

Salido, E. C., Yen, P. H., Koprivnikar, K., Yu, L. C. and Shapiro, L. J. (1992). The human enamel protein gene amelogenin is expressed from both the X and the Y chromosomes. *Am. J. Hum. Genet.* **50**, 303-316.

Sasaki, T., Segawa, K., Takiguchi, R. and Higashi, S. (1984). Intercellular junctions in the cells of the human enamel organ as revealed by freeze-fracture. *Arch. Oral Biol.* **29**, 275-286.

Senoo, M., Pinto, F., Crum, C. P. and McKeon, F. (2007). p63 Is essential for the proliferative potential of stem cells in stratified epithelia. *Cell* **129**, 523-536.

Smith, C. E. and Nanci, A. (1995). Overview of morphological changes in enamel organ cells associated with major events in amelogenesis. *Int. J. Dev. Biol.* **39**, 153-161.

Smyth, G. K. (2004). Linear models and empirical bayes methods for assessing differential expression in microarray experiments. *Stat. Appl. Genet. Mol. Biol.* **3**, Article 3.

Sonnenberg, A. and Liem, R. K. (2007). Plakins in development and disease. *Exp. Cell Res.* **313**, 2189-2203.

Stephanopoulos, G., Garefalaki, M. E. and Lyroudia, K. (2005). Genes and related proteins involved in amelogenesis imperfecta. *J. Dent. Res.* **84**, 1117-1126.

Stephen, L. X., Hamersma, H., Gardner, J. and Beighton, P. (2001). Dental and oral manifestations of sclerosteosis. *Int. Dent. J.* **51**, 287-290.

ten Dijke, P., Krause, C., de Gorter, D. J., Lowik, C. W. and van Bezooijen, R. L. (2008). Osteocyte-derived sclerostin inhibits bone formation: its role in bone morphogenetic protein and Wnt signaling. *J. Bone Joint Surg. Am.* **90 Suppl. 1**, 31-35.

Thesleff, I., Wang, X. P. and Suomalainen, M. (2007). Regulation of epithelial stem cells in tooth regeneration. *C. R. Biol.* **330**, 561-564.

Thomason, H. A., Scothern, A., McHarg, S. and Garrod, D. R. (2010). Desmosomes: adhesive strength and signalling in health and disease. *Biochem. J.* **429**, 419-433.

Truong, A. B., Kretz, M., Ridky, T. W., Kimmel, R. and Khavari, P. A. (2006). p63 regulates proliferation and differentiation of developmentally mature keratinocytes. *Genes Dev.* **20**, 3185-3197.

van Steensel, M. A., Steijlen, P. M., Bladergroen, R. S., Vermeer, M. and van Geel, M. (2005). A missense mutation in the type II hair keratin hHb3 is associated with monilethrix. *J. Med. Genet.* **42**, e19.

Xu, Y., Zhou, Y. L., Luo, W., Zhu, Q. S., Levy, D., MacDougald, O. A. and Snead, M. L. (2006). NF-Y and CCAAT/enhancer-binding protein alpha synergistically activate the mouse amelogenin gene. *J. Biol. Chem.* **281**, 16090-16098.

Yamakoshi, Y., Hu, J. C., Iwata, T., Kobayashi, K., Fukae, M. and Simmer, J. P. (2006). Dentin sialophosphoprotein is processed by MMP-2 and MMP-20 in vitro and in vivo. *J. Biol. Chem.* **281**, 38235-38243.

Yang, A., Kaghad, M., Wang, Y., Gillett, E., Fleming, M. D., Dotsch, V., Andrews, N. C., Caput, D. and McKeon, F. (1998). p63, a p53 homolog at 3q27-29, encodes multiple products with transactivating, death-inducing, and dominant-negative activities. *Mol. Cell* **2**, 305-316.

Yang, A., Schweitzer, R., Sun, D., Kaghad, M., Walker, N., Bronson, R. T., Tabin, C., Sharpe, A., Caput, D., Crum, C. et al. (1999). p63 is essential for regenerative proliferation in limb, craniofacial and epithelial development. *Nature* **398**, 714-718.

Yuasa, K., Fukumoto, S., Kamasaki, Y., Yamada, A., Fukumoto, E., Kanaoka, K., Saito, K., Harada, H., Arikawa-Hirasawa, E., Miyagoe-Suzuki, Y. et al. (2004). Laminin alpha2 is essential for odontoblast differentiation regulating dentin sialoprotein expression. *J. Biol. Chem.* **279**, 10286-10292.

Zhou, Y. L. and Snead, M. L. (2000). Identification of CCAAT/enhancer-binding protein alpha as a transactivator of the mouse amelogenin gene. *J. Biol. Chem.* **275**, 12273-12280.

Zhou, Y. L., Lei, Y. and Snead, M. L. (2000). Functional antagonism between Msx2 and CCAAT/enhancer-binding protein alpha in regulating the mouse amelogenin gene expression is mediated by protein-protein interaction. *J. Biol. Chem.* **275**, 29066-29075.